The influence of residential and workday population mobility on exposure to air pollution in the UK

Stefan Reis[a,b,*], Tomáš Liška[a,c], Massimo Vieno[a], Edward J. Carnell[a], Rachel Beck[a], Tom Clemens[d], Ulrike Dragosits[a], Samuel J. Tomlinson[a], David Leaver[a], Mathew R. Heal[c]

[a] *Centre for Ecology & Hydrology, Bush Estate, Penicuik EH26 0QB, UK*
[b] *University of Exeter Medical School, Knowledge Spa, Truro TR1 3HD, UK*
[c] *School of Chemistry, University of Edinburgh, Joseph Black Building, David Brewster Road, Edinburgh EH9 3FJ, UK*
[d] *Farr Institute, School of GeoSciences, University of Edinburgh, Nine, BioQuarter 9 Little France Road, Edinburgh EH16 4UX, UK*

ARTICLE INFO

ABSTRACT

Traditional approaches of quantifying population-level exposure to air pollution assume that concentrations of air pollutants at the residential address of the study population are representative for overall exposure. This introduces potential bias in the quantification of human health effects. Our study combines new UK Census data comprising information on workday population densities, with high spatio-temporal resolution air pollution concentration fields from the WRF-EMEP4UK atmospheric chemistry transport model, to derive more realistic estimates of population exposure to NO_2, $PM_{2.5}$ and O_3. We explicitly allocated workday exposures for weekdays between 8:00 am and 6:00 pm. Our analyses covered all of the UK at 1 km spatial resolution. Taking workday location into account had the most pronounced impact on potential exposure to NO_2, with an estimated $0.3\,\mu g\,m^{-3}$ (equivalent to 2%) increase in population-weighted annual exposure to NO_2 across the whole UK population. Population-weighted exposure to $PM_{2.5}$ and O_3 increased and decreased by 0.3%, respectively, reflecting the different atmospheric processes contributing to the spatio-temporal distributions of these pollutants. We also illustrate how our modelling approach can be utilised to quantify individual-level exposure variations due to modelled time-activity patterns for a number of virtual individuals living and working in different locations in three example cities. Changes in annual-mean estimates of NO_2 exposure for these individuals were considerably higher than for the total UK population average when including their workday location. Conducting model-based evaluations as described here may contribute to improving representativeness in studies that use small, portable, automatic sensors to estimate personal exposure to air pollution.

1. Introduction

1.1. Background

Traditional approaches to quantifying population-level exposure to air pollution assume that concentrations of air pollutants at the residential address of the study population are representative for overall exposure. However, as early as 1982, Ott highlighted that '*Many previous investigators unfortunately calculate "exposures" by relying on data from fixed air monitoring stations, and they assume that people are located in the same place, usually their residential address, throughout a 24-h period*' (Ott, 1982).

This introduces potential bias in the quantification of human health effects, as the individual and population-level mobility of receptors is not accounted for. The magnitude and direction of this bias is widely discussed in the environmental exposure and health effects literature, primarily from the viewpoint of utilising small, portable air pollution sensors to quantify personal exposure directly on an individual level (Steinle et al., 2013, 2015; Buonanno et al., 2012; Gariazzo et al., 2016; Marek et al., 2016) or mobile devices to assess mobility (Dewulf et al., 2016; Nyhan et al., 2016; Glasgow et al., 2016; Park and Kwan, 2017). While results emerging from these studies are important for understanding the impact of specific mobility patterns (Setton et al., 2008, 2011; Beckx et al., 2009; Dons et al., 2011; Dhondt et al., 2012; Ragettli et al., 2014, 2015; Brokamp et al., 2016; Smith et al., 2016), for exposure in different micro-environments and for the relative contributions of these to overall personal exposure, up-scaling from this individual level to population level exposure is not straightforward.

* Corresponding author at: Centre of Ecology & Hydrology, Bush Estate, Penicuik EH26 0QB, UK.
E-mail address: srei@ceh.ac.uk (S. Reis).

It is in this context that atmospheric chemistry transport models (ACTMs), which have achieved substantial progress in accuracy, can provide consistent spatio-temporal air pollution concentration fields for both individual and population levels of exposure assessment where personal or stationary observations are not available (including for historic and future exposure estimates). In addition, in the United Kingdom (UK) at least, new spatial data on workday location information is available for the first time from the most recent Census. Consequently, the motivation of this paper is to answer the following three research questions:

(1) How does the modelled exposure to key ambient air pollutants differ when comparing use of residential location only with a method accounting for workday location at population level?
(2) To what extent does the spatio-temporal variability of different pollutants affect population exposure regionally?
(3) Can modelled exposure inform the upscaling of personal exposure monitoring results for ambient air pollution?

1.2. Objectives

In this paper, we illustrate the application of a state-of-the-art ACTM with high spatio-temporal resolution for the UK (e.g. Vieno et al., 2010; Vieno et al., 2014; Vieno et al., 2016a,b). We demonstrate how modelled air pollution fields combined with population data, for usual residential and workday locations can give insight into the different exposures to a range of air pollutants. We analyse the estimated population exposure variability between working hours and other times for fine particulate matter ($PM_{2.5}$), nitrogen dioxides (NO_2) and ground-level ozone (O_3). These pollutants have different spatio-temporal variations owing to their different emission sources and different time-scales of atmospheric physicochemical formation and loss processes.

We further evaluate the results of these calculations both at UK population level for total estimated exposure and assess potential exposure variability for selected virtual individuals. For the individual case studies, we assign locations of residence in more or less densely populated parts of a city, and a city centre place of work, and compare the extent of individual potential exposure differences to population level values.

2. Methods

2.1. Population mapping

Fig. 1 illustrates the methodology used to derive the high-resolution population distribution maps. Data on population distribution for both residential and workday for the UK is available to the public from statistical offices in England, Wales, Northern Ireland and Scotland, e.g. via the Office for National Statistics (ONS). The 'workday' population distributions are a new product, derived from the 2011 Census. ONS defines the workday population in a geographical area as "all usual residents aged 16 and above who are in employment and whose workplace is in the area, and all other usual residents of any age who are not in employment but are resident in the area" (ONS, 2014). The geographical areas for which census estimates are provided reflect different levels of administrative boundaries, from Devolved Administration (i.e. England, Wales, Scotland and Northern Ireland) to Output Areas (OA) as the smallest. OAs were introduced in Scotland at the 1981 Census and elsewhere at the 2001 Census. In England and Wales, 2001 Census OAs were based on postcodes (at Census Day) and fit within the boundaries of 2003 statistical wards and parishes. The minimum OA size was 40 resident households and 100 resident people, with recommended sizes being larger at 125 households. As a consequence of size thresholds, small wards and parishes were incorporated into larger OAs.

The OAs are polygons with highly variable sizes and shapes. As the

model output of atmospheric concentrations is provided on a regular grid, the population distribution was mapped onto the same grid for merging with the modelled air pollution concentration fields. This allows for a more uniform spatial analysis based on a regular grid, whereas mapping pollution fields onto OA shapes may lead to spreading pollutant concentrations across larger areas in sparsely populated regions. The dataset used for this study therefore combines 2011 UK Census population data at the OA level with land cover data (Land Cover Map 2015, Rowland et al., 2017). The categories 'Urban' and 'Suburban' were aggregated to create a consistent gridded population data product to provide a population density surface at 1 km × 1 km spatial resolution. The mapping products are based on the British National Grid (OSGB36 datum). The dataset for both residential and workday populations has been published and is publicly available (Reis et al., 2017, https://doi.org/10.5285/0995e94d-6d42-40c1-8ed4-5090d82471e1).

The UK population distribution for both residential (RES) and workday (WD) populations has been mapped, with differences not easy to identify at national scale (see Fig. S1, Suppl. mat.). In particular around urban agglomerations, the full extent of the magnitude and the spatial patterns of workday mobility effects at population level is most appropriately revealed by the difference map displayed in Fig. 2.

The three example magnified maps in Fig. 2a–c highlight that in most cases urban centres gain population during working days due to commuting, while population density in suburbs and rural areas is reduced. The most striking effect is observed for central London (Fig. 2c) where the residential population is comparatively low, compared with the marked increase in workday population. During working hours, population densities exceed 120,000 km^{-2}, with 10 to 20-fold increases in the local population density, for instance, for the City of London.

2.2. Atmospheric modelling

The EMEP4UK model used here for quantifying atmospheric pollutant concentrations is a regional ACTM based on version rv4.10 of the European Monitoring and Evaluation Programme (EMEP) Meteorological Synthesizing Centre - West (MSC-W) model (www.emep.int), which is described in Simpson et al. (2012). A detailed description of the EMEP4UK model is provided in Vieno et al. (2010, 2014, 2016a,b). The model produces hourly concentrations of a wide range of gaseous and particulate matter species.

The EMEP4UK model's meteorological driver is the Weather Research and Forecast (WRF) model version 3.7.1 (Skamarock et al., 2008). The EMEP4UK and WRF model domain uses a one-way nested approach with a latitude/longitude grid at a horizontal resolution of 0.5° × 0.5° (~55.5 km at the equator) for an extended European domain, ~0.055° × ~0.055° (~6.2 km at the equator) for the British Isles nested domain (UK & Republic of Ireland), and ~0.018° × ~0.018° (~2 km at the equator) for the innermost domain covering the United Kingdom. The boundary conditions at the edge of the European domain are prescribed concentrations in terms of latitude and adjusted for each year as described in Simpson et al. (2012).

We used emission data and meteorology for 2015. Land-based anthropogenic emissions for the UK were obtained from the National Atmospheric Emission Inventory (NAEI, http://naei.beis.gov.uk/). Elsewhere, the EMEP emission estimates provided by the Centre for Emission Inventories and Projections (CEIP, http://www.ceip.at/) were used. Estimates for shipping emissions were derived from Jalkanen et al. (2016) and were for the year 2011.

2.3. Population and air pollutant data integration

In order to align the pollutant concentration fields with the population data, the maps of NO_2, $PM_{2.5}$ and O_3 were re-gridded to match the spatial reference system of the population data (OSGB36 datum). This was achieved through the linear re-gridding scheme in the UK Met
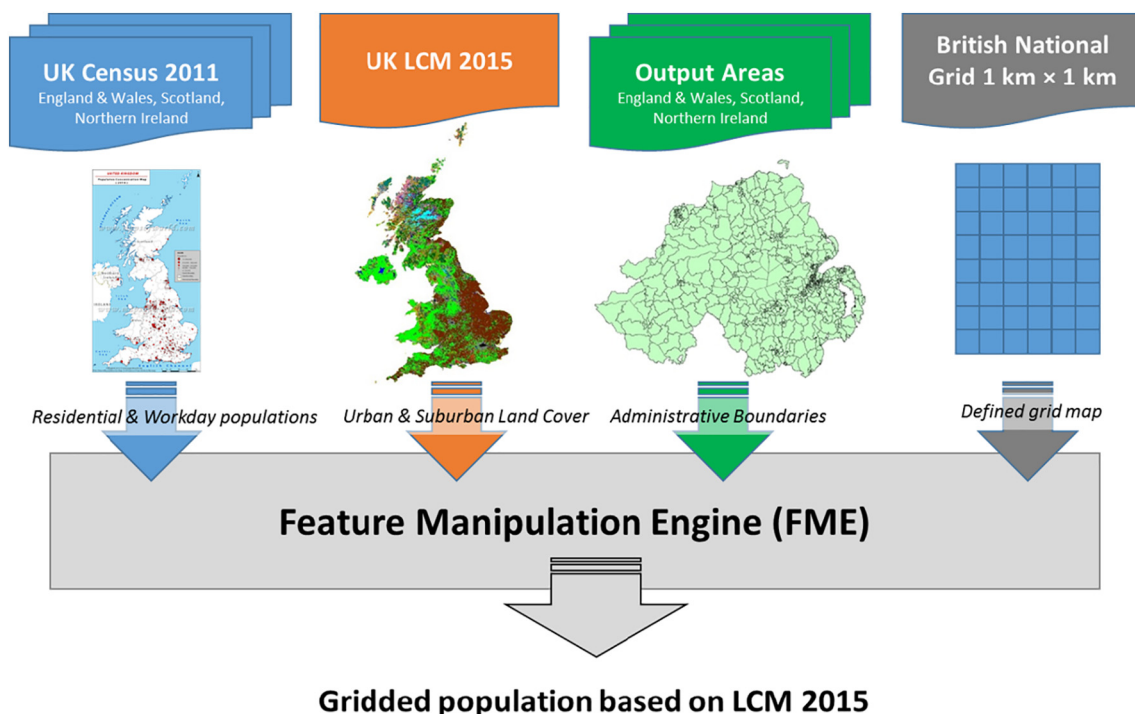
Fig. 1. Flowchart for the production of high resolution population maps (FME © Safe Software; LCM = Land Cover Map).

Office's Iris 1.12 Python library (http://scitools.org.uk/iris/docs/v1.12.0/index.html). The resulting concentration maps are shown in Fig. 3 for all grid cells with a population greater than zero, and illustrate the spatial distributions of these three pollutants. The influence of the urban agglomerations on concentrations are apparent – the spatial patterns in these concentration fields are discussed in Section 3.
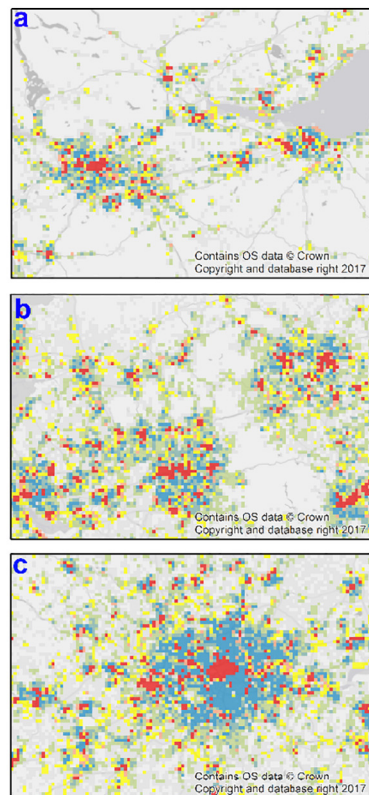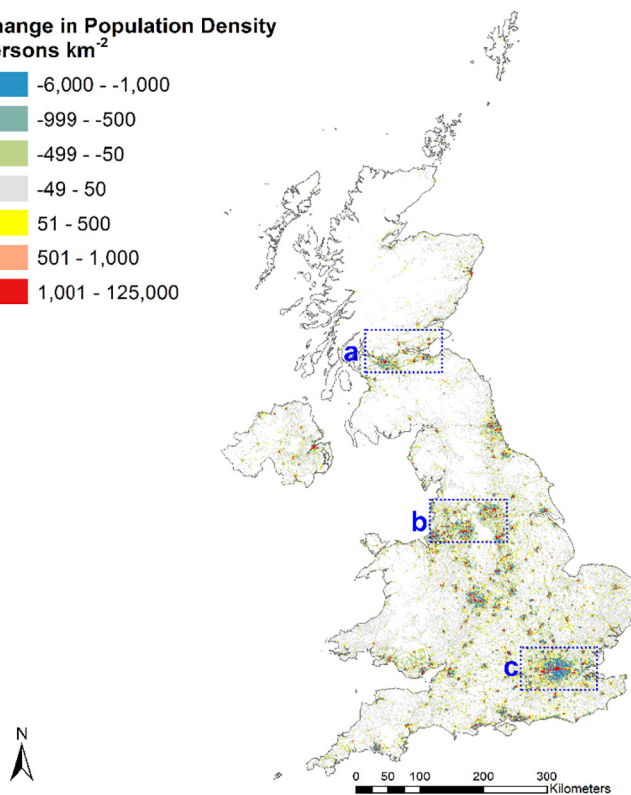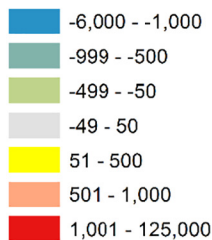

Fig. 2. Difference between UK workday and residential population densities (km^{-2}) (left). Negative values represent a net loss in population during regular working days, while positive values indicate a net gain. Maps a–c are magnifications for the Central Belt of Scotland, the Liverpool-Manchester-Leeds-Sheffield region, and Greater London, respectively.
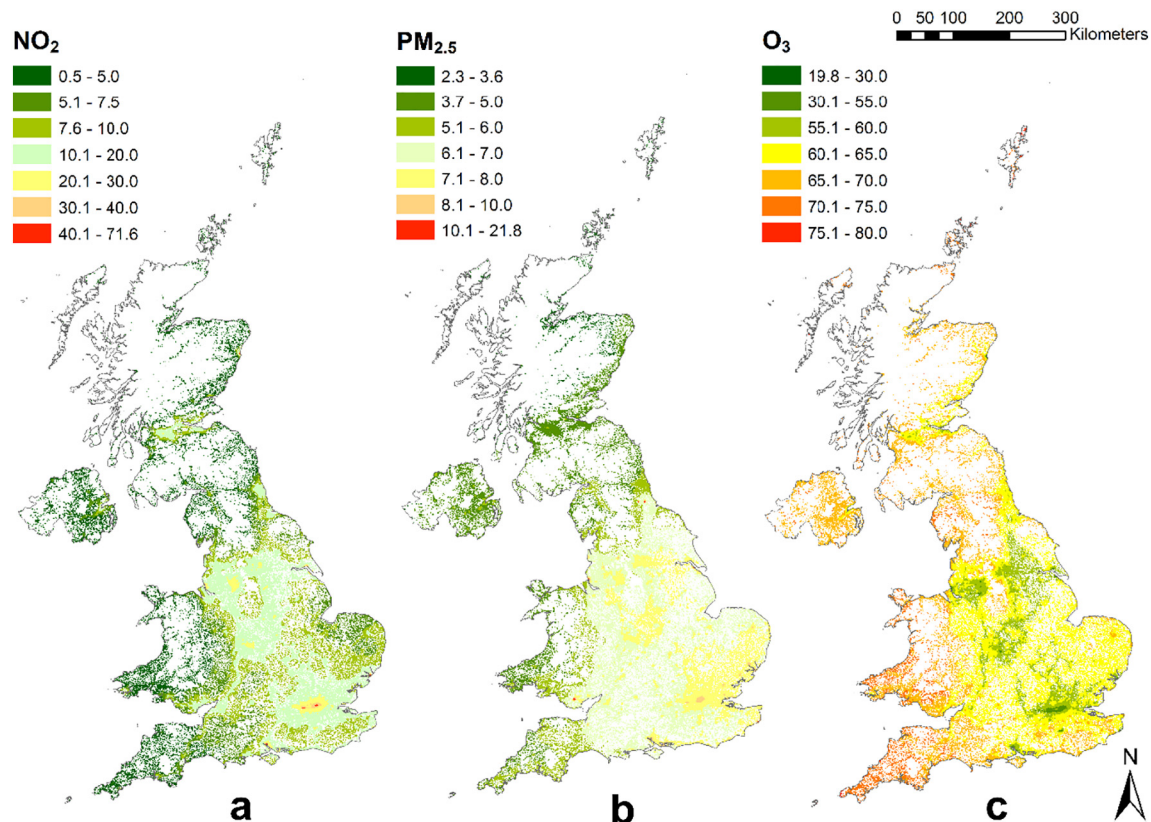
Fig. 3. Modelled annual mean concentration at 1 km × 1 km spatial resolution (see text for details) of NO_2 (a), $PM_{2.5}$ (b) and O_3 (c) for the year 2015 (all units $\mu g\,m^{-3}$). To illustrate the spatial relationship with population distribution, grid cells with no residential or workday populations are shown in white.

2.4. Exposure calculation

Three annual mean population exposures were calculated for each pollutant in each grid cell for each hour of the year: Residential only (RE_i), Workday only (WE_i) and combined Residential-Workday (RWE_i). The RE_i and WE_i exposures represent scenarios in which the whole UK population stays all the time at their place of residence and work, respectively, while the RWE_i represents a more 'realistic' scenario in which people spend some time at home and some time at work. The RE_i and WE_i were calculated as

$$E_i = P_i \times \overline{C}_i \tag{1.1}$$

where E_i (either RE_i for Usual Resident or WE_i for Workday) is the annual mean population exposure in grid cell i, P_i is the respective population number in grid cell i and $\overline{C}_i$ is the annual mean concentration of the pollutant in grid cell i. For the calculation of RWE_i it is assumed that the whole UK population is at their workday locations between 8 am and 6 pm Monday to Friday and at their home at all other times. Clock changes to British Summer Time in March and back to Greenwich Mean Time in October are accounted for, but the 8 days of public holiday in the year are treated as week days. Exposures while in transit and mode of commuting between work and home cannot be explicitly modelled in this population-level study. However, for much of the population the hours assigned here to workday will include transit time spent not at their place of residence. In this model, people are assigned 29.8% of time at their workplace and the rest at home. RWE_i is then calculated as

$$RWE_i = \frac{R_i \times \sum C_{Ri} + W_i \times \sum C_{Wi}}{8760} \tag{1.2}$$

where RWE_i is the combined mean population exposure in grid cell i, R_i is the Usual Resident population in grid cell i, ΣC_{Ri} is the sum of all hourly concentrations of the pollutant in grid cell i outside working hours, W_i is the Workday population in grid cell i, ΣC_{Wi} is the sum of all hourly concentrations of the pollutant in grid cell i during working hours and 8760 is the number of hours in 2015. As the difference between the total Residential and Workday populations in the UK is negligible (minor differences occur due to cross-border and offshore commuting), the population-weighted mean exposure to a pollutant is calculated as

$$\overline{E} = \frac{\sum_{i=1}^{n} E_i}{P} \tag{1.3}$$

where $\overline{E}$ is the population-weighted mean exposure for a population (Usual Resident, Workday, Combined), n is the number of populated grid cells by a population, E_i is the mean exposure in grid cell i for a population and P is the respective total population. Usual Resident population is used for the calculation of $\overline{RWE}$.

2.5. Individual exposure case studies

In addition to the national-scale assessment of the difference in population exposure, we have designed a case study with virtual participants to illustrate how a model-based estimate as discussed in this paper may be used to support the design of personal exposure studies. For this purpose, we spatially allocated pairs of individuals to residential locations in a low and high built-up area respectively in three urban areas from north to south (see Fig. 5). For the pair of individuals in each urban area, the same grid cell was selected for workplace location. The objective of these case studies was to illustrate that differences in individual exposure within small geographic areas could be captured with our modelling approach. We acknowledge, however, that due to the size of 1 km × 1 km grid cells used, actual exposure differences may potentially be much larger.

Table 1
Residential ($\overline{RE}$), Workday ($\overline{WE}$) and combined Residential-Workday ($\overline{RWE}$) population-weighted mean exposure to NO_2, $PM_{2.5}$ and O_3 in the UK. Also shown is the ratio of ($\overline{RWE}/\overline{RE}$).

UK	$\overline{RE}$	$\overline{WE}$	$\overline{RWE}$	$\overline{RWE}/\overline{RE}$
	($\mu g\,m^{-3}$)	($\mu g\,m^{-3}$)	($\mu g\,m^{-3}$)	
NO_2	14.3	15.2	14.6	1.020
$PM_{2.5}$	6.7	6.8	6.7	1.003
O_3	62.3	61.9	62.1	0.997

3. Results

3.1. Population-level assessment of exposure differences

The population-weighted mean exposures to NO_2, $PM_{2.5}$ and O_3 in the UK calculated for each population scenario are shown in Table 1. The results show very small differences between Residential and Workday population-weighted mean exposures to $PM_{2.5}$ and O_3. Therefore accounting for exposure to these pollutants at the place of work results in negligible exposure differences at the population level. However, the results for NO_2 show an increase of $0.9\,\mu g\,m^{-3}$ in the population-weighted mean exposure for the Workday population relative to the Residential population. Consequently, in the combined Residential-Workday population scenario, the population-weighted mean exposure to NO_2 is $0.3\,\mu g\,m^{-3}$ (or 2%) higher than when using residential location only to calculate potential exposure. This impact on population level exposure to NO_2 is about an order of magnitude greater than for $PM_{2.5}$ and O_3 and reflects the much greater spatial gradients in NO_2 concentrations compared with those for $PM_{2.5}$ and O_3 illustrated by the scales of the maps shown in Fig. 3. The map for NO_2 clearly shows that the highest concentrations and gradients of NO_2 are

associated with urban agglomerations. This is due to both the change in location for population during working hours, as well as the temporal patterns of ambient concentration changes. At population level, it is not feasible to quantitatively apportion how the spatial and temporal factors contribute to the variations in overall exposure; this could only be done at individual level and would vary with individual.

The greater effect for NO_2 also reflects the higher temporal variation, in that concentrations of NO_2 are generally higher everywhere during workday hours, and particularly in work place locations (centres of urban areas) precisely because people are working in these locations. The resulting increase in population density in urban centres during working hours leads to a substantial increase in emissions, and in particular NO_2 concentrations from fossil fuel combustion. Road traffic and static combustion are major sources of NO_x (NO and NO_2) and the NO_2 concentrations vary considerably over space and time because of the rapid dispersion and chemical reactions of NO_x – timescales of minutes to a few hours – in particular the reaction between NO and O_3 to form additional NO_2 (Cyrys et al., 2012). Meteorological factors, as well as other aspects (e.g. street canyons resulting in complex air flows), influence the build-up of ambient concentrations and further affect both the spatial and temporal variability.

Table 1 indicates that there is actually a small decrease in potential population-level exposure to ground-level O_3 when taking into account workday population distribution. This is because, as shown in Fig. 3c, O_3 is typically slightly depleted in urban areas and along major road networks. This is the corollary of the reaction between NO and O_3 that leads to enhanced NO_2 in areas of high NO_x emissions simultaneously reducing concentrations of urban O_3. In contrast highest concentrations of O_3 are in the most rural areas, along the west coast in particular for the UK, due to background concentrations stemming from hemispheric transport and higher levels (because of reduced surface deposition) over the sea. However populations are much lower in these areas.
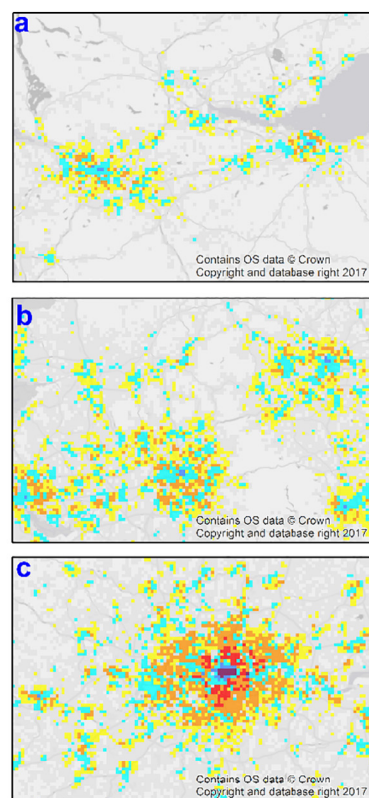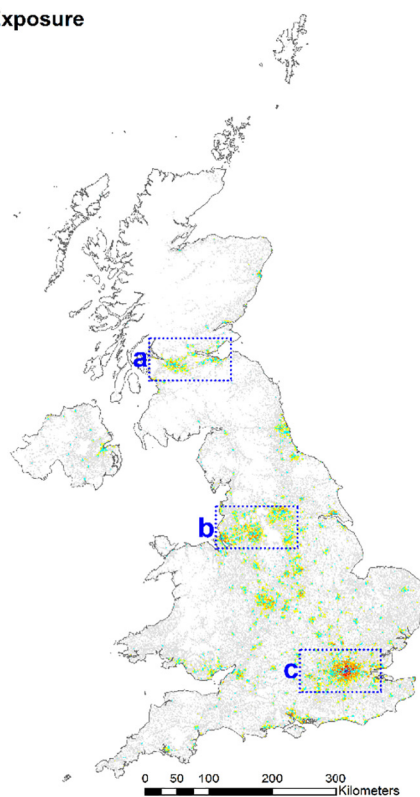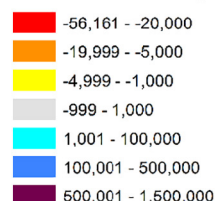

Fig. 4. Comparison of population-weighted concentrations of NO_2 (in $\mu g\,m^{-3} \times$ persons km^{-2}) calculated by using the difference between residential and workday populations (aggregated over all hours of the year, see Section 2.4). Maps a–c are magnifications for the Central Belt of Scotland, the Liverpool-Manchester-Leeds-Sheffield region, and Greater London, respectively.

In the case of PM$_{2.5}$, Fig. 3b shows that PM$_{2.5}$ concentrations exhibit a fairly smooth pattern across the UK, with a declining gradient from the southeast to the northwest. This is caused by the transport of secondary inorganic aerosol and other particles from continental Europe and has been documented for instance by Vieno et al. (2016a,b) and Kiesewetter et al. (2015a,b). Superimposed on this are sources of primary PM$_{2.5}$ emissions in UK urban areas but the proportion of these primary sources to total PM$_{2.5}$ is generally not high which is why there is lower spatial contrasts in PM$_{2.5}$ compared with those for NO$_2$ and consequently why changes in population-level exposure to PM$_{2.5}$ are much smaller than for NO$_2$ when accounting for workday population movement into urban areas (Table 1). Although the magnitude of the increased workday population exposure is smaller for PM$_{2.5}$ than for NO$_2$ the fact that both are increased reflects also the generally high spatial correlation between these two pollutants as shown in Fig. 3a and b.

The impact of taking account of workday population density for NO$_2$ is further emphasised in Fig. 4 which shows the map of population-weighted exposures to NO$_2$ (in $\mu g\,m^{-3} \times persons\,km^{-2}$) calculated from the difference between residential and workday populations integrated over the year. The legend scale of the figure shows that a few grid cells have very large increases in the product of population density and NO$_2$ concentrations, while a larger number of cells have smaller reductions in population-weighted exposure values. This is a consequence of both the accumulation of people in urban centres during working hours and the higher concentrations of NO$_2$ in those urban centres, while lower concentrations in rural and residential areas show smaller reductions in exposure in contrast (see Figs. 2 and 3). Furthermore, Fig. 4 highlights the corresponding changes between areas which are predominantly residential, and others where work places are located. This is visible for all urban areas, but most prominent in the case of the Greater London area (Fig. 4c). Here, the increase for the City of London exhibits by far the largest increase in population-weighted exposure to NO$_2$, reflecting both the substantial increase of population density and the high ambient NO$_2$ concentrations during working hours.

3.2. Case studies of modelled individual-level exposure differences

The previous section indicates a comparatively small population-level difference in exposures to NO$_2$, PM$_{2.5}$ and O$_3$ between solely using residential locations, or accounting for workday locations as well. However, exploratory analysis of the data indicated the potential for rather marked differences in the exposure of individuals commuting into areas where ambient concentrations during working hours are high. To illustrate such differences, we considered three pairs of virtual individuals in each of the Edinburgh, Manchester and London areas with a residential address in either a more or less densely built-up area of their respective cities and a workday location in their city centre. Table 2 describes the categorisation of those residential and workday locations and Fig. 5 provides a geospatial reference for each

Table 2
Categorisation of locations for individual exposure calculation (location names in brackets for reference).

		Edinburgh	Manchester	London
Residential	Low building density	A1 (Gilmerton)	B1 (St. George's Island)	C1 (Southfields)
Residential	High building density	A2 (Drummond Street)	B2 (Didsbury)	C2 (Mayfair)
Workday	City centre	A3 (West End)	B3 (Albert's Square)	C3 (City of London)

location within the three urban areas. As the 1 km × 1 km grid cells comprise mixed land-use categories, the selection was conducted visually based on Open Street Map (www.openstreetmap.org) and aerial photography to identify areas with high vs. low density of building cover. The resulting differences in potential exposure are illustrative for virtual individuals, but not representative for any specific population group. Note that the assignment of high or low building density does not necessarily reflect the radial distance from the urban centre, as the maps in Fig. 5 clearly show.

For each individual, the difference between a residential-only exposure and combined residential and workday exposures was calculated using the same approach as described in Section 2.4. Annual mean concentrations for each individual are displayed in Fig. 6. For NO$_2$, the annual mean concentrations of individuals living in high building density locations is higher than for those living in low building density locations, while the opposite is the case for O$_3$. The individual exposures to annual mean PM$_{2.5}$ differ only marginally, illustrating the comparatively spatially homogeneous PM$_{2.5}$ concentrations and relatively small contributions from local emissions.

Fig. 7 shows the absolute and relative differences in annual mean exposures to the three pollutants between individuals with residential addresses in low building density locations or in high building density locations in the three urban areas. In all cases, the individuals living in the low building density locations had lower annual mean exposure to NO$_2$ than those living in the high building density locations, with absolute NO$_2$ concentration differences ranging from 3.0 $\mu g\,m^{-3}$ in Manchester to 6.3 $\mu g\,m^{-3}$ in Edinburgh and 10.6 $\mu g\,m^{-3}$ in London. Differences in exposure to O$_3$ were smaller and exposure for the individuals living in the less densely built-up locations was higher (0.7, 4.7 and 7.9 $\mu g\,m^{-3}$ respectively). The differences in absolute exposure to PM$_{2.5}$ of virtual individuals were negligible in all three cities (all differences < 0.8 $\mu g\,m^{-3}$), but the figure illustrates the influence of long-range transported fine particles from continental Europe, which diminishes toward the north of the country.

However, Fig. 7 shows that while absolute differences in exposure to NO$_2$ between the two individuals were largest in London, the relative difference in NO$_2$ exposure was greatest in Edinburgh (35% and 25%, for Edinburgh and London, respectively). Similarly, while absolute differences in exposure to PM$_{2.5}$ between the two individuals in each city were small, the relative differences were 8.3%, 9.1% and 1.4%, respectively, for the London, Edinburgh and Manchester examples. A likely explanation for this can be found in the spatial configuration of Edinburgh, which is less densely built-up without street canyons and traffic volumes comparable to London. This leads to lower background NO$_2$ concentrations across the centre of Edinburgh and more pronounced variations between parts of the city within a small area.

4. Discussion

To our knowledge, this is the first time that the impact of workday population mobility has been investigated at country scale for the UK and based on routinely collected CENSUS data products. Some previous papers have investigated differences at country scale based on modelled data (e.g. for the Netherlands by Beckx et al., 2009), as well as for individual-level exposures. In a study with some parallels to ours, but for a much smaller area, Park and Kwan (2017) demonstrated the importance to exposure assessment of air pollution in Los Angeles County of considering both the spatio-temporal variability of O$_3$ and individual daily movement patterns. They found significant differences across four different types of exposure estimates: individual movement data and hourly air pollution concentrations; individual movement data and daily average air pollution data; residential location and hourly pollution levels; and residential location and daily average pollution data. Similarly, Setton et al. (2011) compared exposure estimates in Vancouver, British Columbia, and Southern California, using paired residence- and mobility-based estimates of individual exposure to
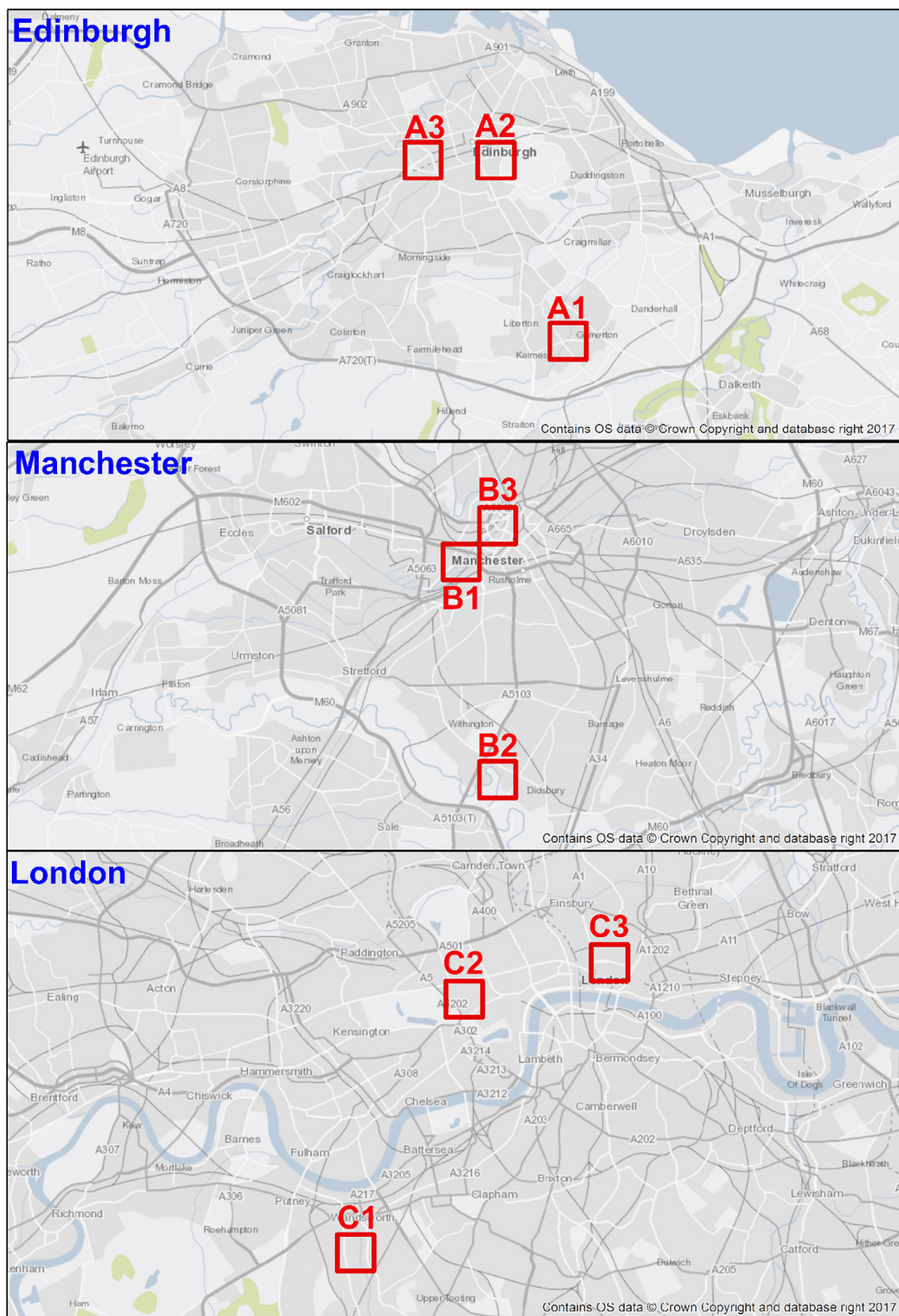
Fig. 5. Location of 1 km × 1 km grid cells selected for model assessment of virtual individuals living in either a low building density (1) or a high building density (2) area and working in a city centre (3) location in Edinburgh (A1–A3), Manchester (B1–B3) and London (C1–C3) (see Table 2 for a description of the individual locations).
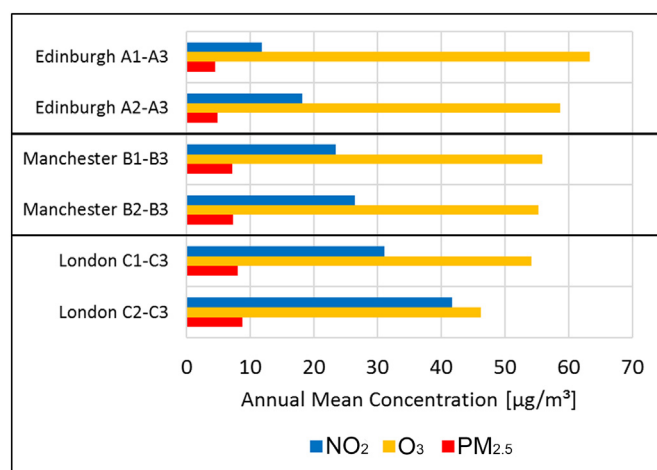
Fig. 6. Comparison of annual mean concentrations for NO_2, O_3 and $PM_{2.5}$ experienced by virtual individuals living in more and less densely built-up locations, respectively, and working in the city centres of Edinburgh, Manchester and London. Each graph illustrates a direct comparison between a residential location and the workday location in each of the cities, for example, a person living in location A1 and working in location A3 in the case of Edinburgh (see Fig. 5 for the spatial context on locations compared).
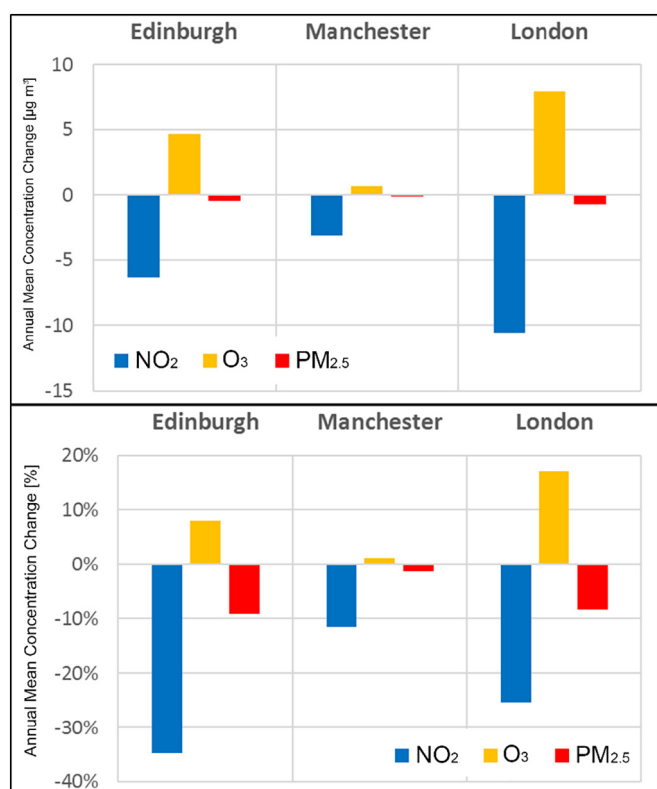

Fig. 7. Absolute (top) and relative (bottom) differences in annual mean concentrations for NO_2, O_3 and $PM_{2.5}$ - expressed as the difference in $\mu g\,m^{-3}$ and in percent - experienced by individuals living in lower density building and higher density building locations, respectively, and working in the city centres of Edinburgh, Manchester and London (see Fig. 5 for details on locations compared).

ambient NO_2. They applied error theory to calculate bias for scenarios when mobility is not considered, and concluded that ignoring daily mobility patterns may contribute to bias toward the null hypothesis in epidemiological studies using individual-level exposure estimates. Likewise, Nyhan et al. (2016) compared population-weighted exposure

to $PM_{2.5}$, in New York City (NYC) both as "Active Population Exposure" (using population activity patterns and spatio-temporal $PM_{2.5}$ concentration levels) and "Home Population Exposure" (assuming a static population distribution as per Census data). They reported that population-weighted exposure for the "Active" scenario was statistically significantly different to the "Home" scenario for most NYC districts. Our simulations of example individual potential exposure estimates presented in Section 3.2 are in line with the conclusions of these previous studies. de Nazelle et al. (2009) investigated simulated population exposure variations as a consequence of changes in mobility patterns in pedestrian-friendly urban designs and found that PM_{10} and O_3 inhalation increased. In a study in Barcelona, Spain, using smartphones to track individual mobility patterns, de Nazelle et al. (2013) reported that average travel activities accounted for 6% of people's time, but contributed to 24% of their daily inhaled dose of NO_2.

Our study has highlighted the importance of a holistic approach to consideration of the impacts on population mobility on exposure to air pollution. Changes in exposure to O_3 are in the opposite direction to NO_2 and $PM_{2.5}$ because of the tendency for O_3 to be higher in rural areas and lower in urban areas. This is important in the context of designing effective interventions (Section 4.1).

The use of small, portable, automatic sensors to estimate personal exposure to air pollution has become quite widespread (Steinle et al., 2013, 2015; Buonanno et al., 2012; Gariazzo et al., 2016; Marek et al., 2016), but although providing opportunities for synergistic monitoring of other relevant parameters, e.g. individual activity levels (Laeremans et al., 2017), such studies are expensive and time consuming. Conducting model-based evaluations similar to those described here in preparation of such sensor-based field studies may contribute to a substantial de-risking and improved representativeness as a result. The illustrative model-based assessment of 'personal' exposure levels for selected individuals demonstrated in Section 3.2 illustrates, how a physical personal exposure monitoring study could be tested ex ante to evaluate aspects of representativeness or the coverage of pollution hotspots, which may not be evident based on sparse fixed monitoring network data only.

Our estimate of a $0.3\,\mu g\,m^{-3}$ increase in population-weighted annual mean exposure to NO_2 when including workday population distributions may appear small but applies to the total UK population of 63.2 million. For long-term exposure to NO_2, the WHO HRAPIE project (WHO, 2013) estimated a relative risk for mortality of 1.055 (95% CI 1.031–1.080) per $10\,\mu g\,m^{-3}$ increase in concentration, as derived from a meta-analysis of relevant studies by Hoek et al. (2013). Taking the central estimate for the relative risk coefficient, our estimate of a $0.3\,\mu g\,m^{-3}$ increase in exposure to NO_2 equates to an increased risk to mortality of 1.0017, or 0.17%. Based on an annual UK mortality of nearly 600,000 (ONS) the additional estimated NO_2 exposure including workplace mobility may contribute to approximately 1000 premature mortalities per year across the UK. The WHO noted that the relative risk assigned to NO_2 may include some of the effects due to $PM_{2.5}$, whose concentrations are often correlated with those of NO_2 and therefore difficult to separate in epidemiological studies. An effects overlap of around 30% (WHO, 2013) would reduce the NO_2-atrributable estimates of premature mortality by a corresponding proportion. However, part of this reduction would be offset in our analyses by the attributable premature mortality associated with the small increase in potential annual mean exposure to $PM_{2.5}$ for which there is also a significant relative risk: COMEAP (2010) estimated a relative risk for all-cause mortality from long-term exposure to $PM_{2.5}$ of 1.06 (95% CI 1.01–1.12) per $10\,\mu g\,m^{-3}$ increase in concentration.

4.1. Outlook and next steps

Beyond the results of this study, the case for taking account of the time-activity patterns and commuting behaviour of individuals or population sub-groups can be made in support of the ex-ante assessment
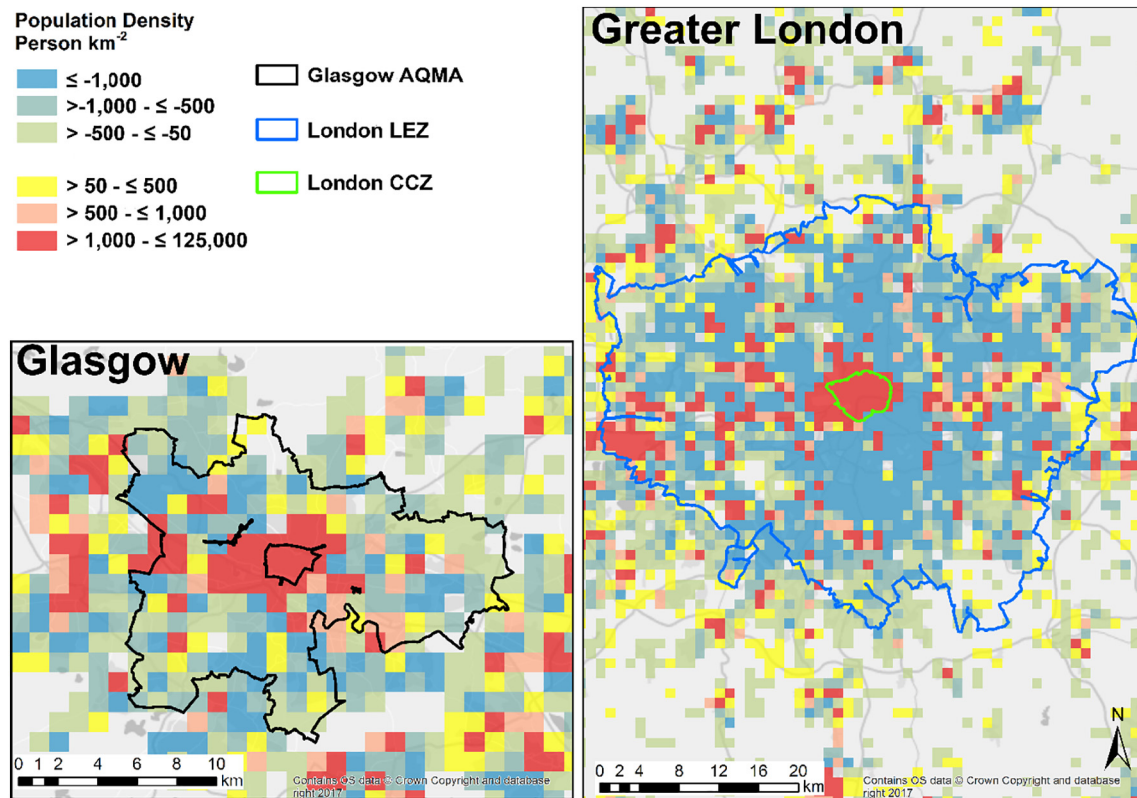
Fig. 8. Implications of differences between workday and residential population densities for the design of air quality interventions depicted by the current Air Quality Management Area (AQMA) for Glasgow (left) and the existing Congestion Charge Zone (CCZ), as well as the Low Emission Zone (LEZ) In the Greater London area (right).

of policy interventions. For example, assessment of boundaries for Air Quality Management Areas (AQMAs) and Low Emission Zones (LEZs) should account for workday population density, as illustrated by Fig. 8. In general, interventions with a focus on achieving compliance with air quality limit values at a small number of existing air quality monitoring sites cannot be expected to automatically achieve the most effective reductions in population exposures and hence a substantial improvement of public health.

The analyses discussed in this paper highlight the different impacts on potential population exposure to NO_2, $PM_{2.5}$ and O_3 when considering workday population distributions in conjunction with different spatio-temporal patterns of these pollutants. It is important to recognise that interventions aiming at the reduction of one pollutant may not deliver improvements for other pollutants by default. For example, reductions of NO_x emissions to lower NO_2 concentrations will likely lead to increases in ambient O_3 locally.

Steps to build upon the approach presented here could focus on several areas.

(1) A more explicit and detailed consideration of commuting patterns, transport modes and time-activity spent in transit will be feasible for particular regions or urban environments, e.g. based on data on the *Location of usual residence and place of work by method of travel to work* (NOMIS, 2014). This may require access to individual-level data on mobility and commuting choice and hence need a safe haven environment in which to work with potentially disclosive datasets. Shekarrizfard et al. (2017) demonstrate such an approach for the Montreal metropolitan area and Int Panis (2010) highlight the benefits of taking activity patterns into account for epidemiological studies. Alternatively, virtual population data emulating real commuting and mobility patterns can be generated from disclosive individual data in order to conduct ex ante model assessments of

interventions (de Nazelle et al., 2009, 2013; Nowok et al., 2016; Raab et al., 2017). This is a viable approach because the effectiveness of interventions does not rely on individual effects, but is evaluated against sub-population level exposure reductions.

(2) Modelling cohorts or vulnerable sub-sets of the total population, e.g. patients suffering from respiratory or cardiovascular diseases and subject to close surveillance in order to combine individual-level monitoring with space-time modelling of environmental exposures. Valero et al. (2009) and Schembari et al. (2013) illustrate the specific need for detailed exposure assessments on the example of individual exposure patterns of pregnant women. In this context, modelled data can enhance real-time monitoring approaches such as described by Marek et al. (2016), utilising Internet of Things concepts. Reis et al. (2015) make a case for better integration of modelling and sensors and provide an in-depth discussion of potential pathways to achieve this.

(3) Further detail may include the 'Location of usual residence and place of work (OA level)' dataset (NOMIS, 2011), derived from Census 2011 data, which would allow for residential and workday population level exposure differences at the OA scale.

Our results illustrate that, when assessing population-level potential exposure to air pollution, accounting for location is less relevant than for individual exposure assessment. In specific contexts, however, for instance at the level of a large conurbation, Oxley et al. (2015) illustrate how assessing both the temporal variations in ambient concentrations of air pollution and the mobility of residential and working populations can lead to substantial differences in the estimates of life expectancy gains. In that way, modelling air pollution at both high spatial and temporal resolution could contribute essential environmental data to the 'daycourse of place' framework developed by Vallee (2017) and support a more explicit assessment of the 'social and political rhythms

of places over a 24-h period and their effects on health inequalities'. Overall, our work contributes to the discussion on the fusion of environmental and health data (Kanjo et al., 2018).

4.2. Conclusions

Our study demonstrates the utility of using new UK Census products comprising information on workday population densities, in combination with high spatio-temporal resolution atmospheric model output, to derive more realistic estimates of population exposure to air pollution. We explicitly allocated workday exposures for weekdays between 8 am and 6 pm. Our analyses covered all of the UK at 1 km spatial resolution. Taking workday location into account had the largest impact on potential exposure to NO_2, with an estimated $0.3\,\mu g\,m^{-3}$ (equivalent to 2%) increase in population-weighted annual exposure to NO_2 across the whole population of the UK. Population-weighted exposure to $PM_{2.5}$ and O_3 increased and decreased by 0.3%, respectively, when including workday population distribution, reflecting the different atmospheric processes contributing to the spatio-temporal distributions of these three pollutants. These findings are in line with other studies, which identified that accounting for a combination of temporal and micro-environmental adjustments led to the most pronounced contrasts in population level and individual exposure.

We also illustrate how the modelling approach applied in this study can be utilised to quantify individual-level exposure variations due to modelled time-activity patterns for a number of virtual individuals living and working in different locations in three example cities. Changes in annual-mean estimates of NO_2 exposure with inclusion of workday location are considerably higher than the population average. The increase in exposure to $PM_{2.5}$ for these virtual individuals was smaller than for NO_2 but still several percent. Conducting model-based evaluations as described here may contribute to improving representativeness in studies that use small, portable, automatic sensors to estimate personal exposure to air pollution by identifying areas and study populations prior to launching field experiments.

The approach presented here can be expanded in several directions, including more explicit modelling of the mode of transport and time spent indoors and outdoors, a focus on particular population sub-groups and better integration of model and sensor and remote-sensing data. In this study, only single pollutant exposure has been considered. One advantage of using modelled data allow for a spatio-temporally explicit quantification of multi-pollutant exposure. This enables the detection of hotspot locations where several pollutants contribute to local exposure risks, and hence a better assessment of health risks in mobile populations.

Supplementary data to this article can be found online at https://doi.org/10.1016/j.envint.2018.10.005.

Acknowledgements

Declaration of interests

The authors declare no competing financial interests.

References

Beckx, C., Int Panis, L., Uljee, I., Arentze, T., Janssens, S., Wets, G., 2009. Disaggregation of nation-wide dynamic population exposure estimates in the Netherlands: applications of activity-based transport models. Atmos. Environ. 43 (34), 5454–5462. https://doi.org/10.1016/j.atmosenv.2009.07.035.

Brokamp, C., LeMasters, G.K., Ryan, P.H., 2016. Residential mobility impacts exposure assessment and community socioeconomic characteristics in longitudinal epidemiology studies. J. Expo. Sci. Environ. Epidemiol. 26, 428–434.

Buonanno, G., Stabile, L., Morawska, L., 2012. Personal exposure to ultrafine particles: the influence of time-activity patterns. Sci. Total Environ. 468–469, 903–907.

COMEAP, 2010. The Mortality Effects of Long-term Exposure to Particulate Air Pollution in the United Kingdom. UK Department of Health Committee on the Medical Effects of Air Pollutants978-0-85951-685-3. http://comeap.org.uk/documents/reports.html (Last Access: 10/03/2018).

Cyrys, J., Eeftens, M., Heinrich, J., Ampe, C., Armengaud, A., Beelen, R., Bellander, T., Beregszaszi, T., Birk, M., Cesaroni, G., Cirach, M., de Hoogh, K., De Nazelle, A., de Vocht, F., Declercq, C., Dedele, A., Dimakopoulou, K., Eriksen, K., Galassir, C., Grauleviciene, R., Grivas, G., Gruzieva, O., Gustafsson, A.H., Hoffmann, B., Iakovides, M., Ineichen, A., Kramer, U., Lanki, T., Lozano, P., Madsen, C., Meliefste, K., Modig, L., Moelter, A., Mosler, G., Nieuwenhuijsen, M., Nonnemacher, M., Oldenwening, M., Peters, A., Pontet, S., Probst-Hensch, N., Quass, U., Raaschou-Nielsen, O., Ranzi, A., Sugiri, D., Stephanou, E.G., Taimisto, P., Tsai, M.Y., Vaskovi, E., Villani, S., Wang, M., Brunekreef, B., Hoek, G., 2012. Variation of NO_2 and NO_x concentrations between and within 36 European study areas: results from the ESCAPE study. Atmos. Environ. 62, 374–390.

de Nazelle, A., Rodriguez, D.A., Crawford-Brown, D., 2009. The built environment and health: impacts of pedestrian-friendly designs on air pollution exposure. Sci. Total Environ. 407, 2525–2535.

de Nazelle, A., Seto, A., Donaire-Gonzalez, D., Mendez, M., Matamala, J., Nieuwenhuijsen, M.J., Jerrett, M., 2013. Improving estimates of air pollution exposure through ubiquitous sensing technologies. Environ. Pollut. 176, 92–99.

Dewulf, B., Neutens, T., Lefebvre, W., Seynaeve, G., Vanpoucke, C., Beckx, C., Van de Weghe, N., 2016. Dynamic assessment of exposure to air pollution using mobile phone data. Int. J. Health Geogr. 15, 14. https://doi.org/10.1186/s12942-016-0042-z.

Dhondt, S., Beckx, C., Degraeuwe, B., Lefebvre, W., Kochan, B., Bellemans, T., Int Panis, L., Macharis, C., Putman, K., 2012. Integration of population mobility in the evaluation of air quality measures on local and regional scales. Atmos. Environ. 59, 67–74. https://doi.org/10.1016/j.atmosenv.2012.04.055.

Dons, D., Int Panis, L., Van Poppel, M., Theunis, J., Willems, H., Torfs, R., Wets, G., 2011. Impact of time–activity patterns on personal exposure to black carbon. Atmos. Environ. 45 (21), 3594–3602. https://doi.org/10.1016/j.atmosenv.2011.03.064.

Gariazzo, C., Pelliccioni, A., Bolignano, A., 2016. A dynamic urban air pollution population exposure assessment study using model and population density data derived by mobile phone traffic. Atmos. Environ. 131, 289–300.

Glasgow, M.L., Rudra, C.B., Yoo, E.H., Demirbas, M., Merriman, J., Nayak, P., Crabtree-Ide, C., Szpiro, A.A., Rudra, A., Wactawski-Wende, J., Mu, L.N., 2016. Using smartphones to collect time-activity data for long-term personal-level air pollution exposure assessment. J. Expo. Sci. Environ. Epidemiol. 26, 356–364.

Hoek, G., Krishnan, R.M., Beelen, R., Peters, A., Ostro, B., Brunekreef, B., Kaufman, J.D., 2013. Long-term air pollution exposure and cardio-respiratory mortality: a review. Environ. Health 12, 43. https://doi.org/10.1186/1476-069X-12-43.

Int Panis, L., 2010. New directions: air pollution epidemiology can benefit from activity-based models. Atmos. Environ. 44 (7), 1003–1004. https://doi.org/10.1016/j.atmosenv.2009.10.047.

Jalkanen, J.P., Johansson, L., Kukkonen, J., 2016. A comprehensive inventory of ship traffic exhaust emissions in the European sea areas in 2011. Atmos. Chem. Phys. 16, 71–84. https://doi.org/10.5194/acp-16-71-2016.

Kanjo, E., Younis, E.M.G., Sherkat, N., 2018. Towards unravelling the relationship between on-body, environmental and emotion data using sensor information fusion approach. Inform. Fusion 40, 18–31.

Kiesewetter, G., Schöpp, W., Heyes, C., Amann, M., 2015a. Modelling PM2.5 impact indicators in Europe: health effects and legal compliance. Environ. Model. Softw. 74, 201–211. https://doi.org/10.1016/j.envsoft.2015.02.022.

Kiesewetter, G., Borken-Kleefeld, J., Schöpp, W., Heyes, C., Thunis, P., Bessagnet, B., Terrenoire, E., Fagerli, H., et al., 2015b. Modelling street level PM10 concentrations across Europe: source apportionment and possible futures. Atmos. Chem. Phys. 15 (3), 1539–1553. https://doi.org/10.5194/acp-15-1539-2015.

Laeremans, M., Dons, E., Avila-Palencia, I., Carrasco-Turigas, G., Orjuela, J.P., Anaya, E., Brand, C., Cole-Hunter, T., de Nazelle, A., Goetschi, T., Kahlmeier, S., Nieuwenhuisen, M., Standaert, A., De Boever, P., Int Panis, L., 2017. Physical activity and sedentary behaviour in daily life: a comparative analysis of the Global Physical Activity Questionnaire (GPAQ) and the SenseWear armband. PLoS ONE 12 (5), e0177765.

Marek, L., Campbell, M., Epton, M., Storer, M., Kingham, S., 2016. Real-time environmental sensors to improve health in the sensing city. Int. Arch. Photogramm. 41, 729–733.

NISRA, 2018. https://www.nisra.gov.uk/statistics/census (Last Access: 06/01/2018).

NOMIS, 2011. Location of usual residence and place of work (OA level). https://www.nomisweb.co.uk/census/2011/wf01bew (Last Access: 06/01/2018).

NOMIS, 2014. Location of usual residence and place of work by method of travel to work. https://www.nomisweb.co.uk/census/2011/wu03uk (Last Access: 06/01/2018).

Nowok, B., Raab, G., Dibben, C., 2016. *synthpop*: bespoke creation of synthetic data in R. J. Stat. Softw. 74 (1), 1–26. https://doi.org/10.18637/jss.v074.i11.

Nyhan, M., Grauwin, S., Britter, R., Misstear, B., McNabola, A., Laden, F., Barrett, S.R.H., Ratti, C., 2016. "Exposure track" - the impact of mobile-device-based mobility patterns on quantifying population exposure to air pollution. Environ. Sci. Technol. 50, 9671–9681.

ONS, 2014. 2011 Census Glossary of Terms. www.ons.gov.uk/ons/guide...definitions/2011-census-glossary.pdf (Last Access: 06/01/2018).

ONS, 2018. https://www.nomisweb.co.uk/census/2011/workday_population (Last Access: 06/01/2018).

Ott, W.R., 1982. Concepts of human exposure to air pollution. Environ. Int. 7 (3), 179–196. https://doi.org/10.1016/0160-4120(82)90104-0.

Oxley, T., ApSimon, H.M., de Nazelle, A., 2015. Investigating the sensitivity of health benefits to focussed PM$_{2.5}$ emission abatement strategies. Environ. Model. Softw. 74, 268–283.

Park, Y.M., Kwan, M.P., 2017. Individual exposure estimates may be erroneous when spatiotemporal variability of air pollution and human mobility are ignored. Health Place 43, 85–94.

Raab, G., Nowok, B., Dibben, C., 2017. Practical data synthesis for large samples. J. Priv. Confid. 7 (3), 67–97.

Ragettli, M.S., Tsai, M.-Y., Braun-Fahrländer, C., de Nazelle, D., Schinder, C., Ineichen, A., Ducret-Stich, R.E., Perez, L., Probst-Hensch, N., Kuenzli, N., Phuleria, H.C., 2014. Simulation of population-based commuter exposure to NO$_2$ using different air pollution models. Int. J. Environ. Res. Public Health 11 (5), 5049–5068. https://doi.org/10.3390/ijerph110505049.

Ragettli, M.S., Phuleria, H.C., Tsai, M.-Y., Schindler, C., de Nazelle, A., Ducret-Stich, R.E., Ineichen, A., Perez, L., Braun-Fahrländer, C., Probst-Hensch, N., Künzli, N., 2015. The relevance of commuter and work/school exposure in an epidemiological study on traffic-related air pollution. J. Expo. Sci. Environ. Epidemiol. 25, 474–481.

Reis, S., Liska, T., Steinle, S., Carnell, E., Leaver, D., Roberts, E., Vieno, M., Beck, R., Dragosits, U., 2017. UK Gridded Population 2011 based on Census 2011 and Land Cover Map 2015. NERC Environmental Information Data Centre https://doi.org/10.5285/0995e94d-6d42-40c1-8ed4-5090d82471e1.

Reis, S., Seto, E., Northcross, A., Quinn, N.W., Convertino, M., Jones, R.L., Maier, H.R., Schlink, U., Steinle, S., Vieno, M., Wimberly, M.C., 2015. Integrating modelling and smart sensors for environmental and human health. Environ. Model. Softw. 74, 238–246. https://doi.org/10.1016/j.envsoft.2015.06.003.

Rowland, C.S., Morton, R.D., Carrasco, L., McShane, G., O'Neil, A.W., Wood, C.M., 2017. Land Cover Map 2015 (Vector, GB). NERC Environmental Information Data Centre https://doi.org/10.5285/6c6c9203-7333-4d96-88ab-78925e7a4e73.

Schembari, A., Triguero-Mas, M., de Nazelle, A., Dadvand, P., Vrijheid, M., Cirach, M., Martinez, D., Figueras, F., Querol, X., Basagaña, X., Eeftens, M., Meliefste, K., Nieuwenhuijsen, M.J., 2013. Personal, indoor and outdoor air pollution levels among pregnant women. Atmos. Environ. 64, 287–295.

Scotland's Census, 2018. http://www.scotlandscensus.gov.uk/ (Last Access: 06/01/2018).

Setton, E.M., Keller, C.P., Cloutier-Fisher, D., Hystad, P.W., 2008. Spatial variations in estimated chronic exposure to traffic-related air pollution in working populations: a simulation. Int. J. Health Geogr. 7, 39. https://doi.org/10.1186/1476-072X-7-39.

Setton, E., Marshall, J.D., Brauer, M., Lundquist, K.R., Hystad, P., Keller, P., Cloutier-Fisher, D., 2011. The impact of daily mobility on exposure to traffic-related air pollution and health effect estimates. J. Expo. Sci. Environ. Epidemiol. 21, 42–48.

Shekarrizfard, M., Faghih-Imani, A., Tetreault, L.F., Yasmin, S., Reynaud, F., Morency, P.,

Plante, C., Drouin, L., Smargiassi, A., Eluru, N., Hatzopoulou, M., 2017. Regional assessment of exposure to traffic-related air pollution: impacts of individual mobility and transit investment scenarios. Sustain. Cities Soc. 29, 68–76.

Simpson, D., Benedictow, A., Berge, H., Bergström, R., Emberson, L.D., Fagerli, H., Flechard, C.R., Hayman, G.D., Gauss, M., Jonson, J.E., Jenkin, M.E., Nyíri, A., Richter, C., Semeena, V.S., Tsyro, S., Tuovinen, J.P., Valdebenito, Á., Wind, P., 2012. The EMEP MSC-W chemical transport model - technical description. Atmos. Chem. Phys. 12, 7825–7865. https://doi.org/10.5194/acp-12-7825-2012.

Skamarock, W.C., Klemp, J.B., Dudhia, J., Gill, D.O., Barker, D.M., Duda, M.G., Huang, X.-Y., Wang, W., Powers, J.G., 2008. A Description of the Advanced Research WRF Version 3. NCAR Technical Note NCAR/TN-475 + STR. https://doi.org/10.5065/D68S4MVH.

Smith, J.D., Mitsakou, C., Kitwiroon, N., Barratt, B.M., Walton, H.A., Taylor, J.G., Anderson, H.R., Kelly, F.J., Beevers, S.D., 2016. The London Hybrid Exposure Model (LHEM): improving human exposure estimates to NO$_2$ and PM$_{2.5}$ in an urban setting. Environ. Sci. Technol. 50 (21), 11760–11768.

Steinle, S., Reis, S., Sabel, C., 2013. Quantifying human exposure to air pollution - moving from static monitoring to spatio-temporally resolved personal exposure assessment. Sci. Total Environ. 443, 184–193.

Steinle, S., Reis, S., Sabel, C., Semple, S., Twigg, M.M., Braban, C.F., Leeson, A.E., Heal, M.R., Harrison, D., Lin, C., Wu, H., 2015. Personal exposure monitoring of PM2.5 in indoor and outdoor microenvironments. Sci. Total Environ. 508, 383–394. https://doi.org/10.1016/j.scitotenv.2014.12.003.

Valero, N., Aguilera, I., Llop, S., Esplugues, A., de Nazelle, A., Ballester, F., Sunyer, J., 2009. Concentrations and determinants of outdoor, indoor and personal nitrogen dioxide in pregnant women from two Spanish birth cohorts. Environ. Int. 35, 1196–1201.

Vallee, J., 2017. The daycourse of place. Soc. Sci. Med. 194, 177–181.

Vieno, M., Dore, A.J., Stevenson, D.S., Doherty, R., Heal, M.R., Reis, S., Hallsworth, S., Tarrason, L., Wind, P., Fowler, D., Simpson, D., Sutton, M.A., 2010. Modelling surface ozone during the 2003 heat-wave in the UK. Atmos. Chem. Phys. 10, 7963–7978. https://doi.org/10.5194/acp-10-7963-2010.

Vieno, M., Heal, M.R., Hallsworth, S., Famulari, D., Doherty, R.M., Dore, A.J., Tang, Y.S., Braban, C.F., Leaver, D., Sutton, M.A., Reis, S., 2014. The role of long-range transport and domestic emissions in determining atmospheric secondary inorganic particle concentrations across the UK. Atmos. Chem. Phys. 14, 8435–8447. https://doi.org/10.5194/acp-14-8435-2014.

Vieno, M., Heal, M., Twigg, M., MacKenzie, I., Braban, C., Lingard, J., Ritchie, S., Beck, R., Móring, A., Ots, R., Di Marco, C., Nemitz, E., Sutton, M.A., Reis, S., 2016a. The UK particulate matter air pollution episode of March–April 2014: more than Saharan dust. Environ. Res. Lett. 11, 044004.

Vieno, M., Heal, M.R., Williams, M.L., Carnell, E.J., Nemitz, E., Stedman, J.R., Reis, S., 2016b. The sensitivities of emissions reductions for the mitigation of UK PM2.5. Atmos. Chem. Phys. 16, 265–276. https://doi.org/10.5194/acp-16-265-2016.

WHO, 2013. Health risks of air pollution in Europe - HRAPIE Project. World Health Organisation, Copenhagen, Denmark http://www.euro.who.int/en/health-topics/environment-and-health/air-quality/publications/2013/health-risks-of-air-pollution-in-europe-hrapie-project-recommendations-for-concentrationresponse-functions-for-costbenefit-analysis-of-particulate-matter,-ozone-and-nitrogen-dioxide (Last Access: 10/03/2018).